EXTRACTION OF AN AVALANCHE DIODE NOISE MODEL FOR ITS APPLICATION AS AN ON-WAFER NOISE SOURCE

M. C. Maya, A. Lázaro, and L. Pradell
Universitat Politècnica de Catalunya (UPC)
Dept. TSC, Campus Nord UPC
Mòdul D3, 08034, Barcelona, Spain

Received 7 January 2003

ABSTRACT: *This paper presents a method to characterize the excess noise ratio (ENR) of an unmatched avalanche noise diode for application as an on-wafer noise source. It is based on the determination of a broadband device noise circuit-model from its measured reflection coefficient and noise powers. Measured ENR is used to calibrated a noise receiver up to 40 GHz.* © 2003 Wiley Periodicals, Inc. Microwave Opt Technol Lett 38: 89–92, 2003; Published online in Wiley InterScience (www.interscience.wiley.com). DOI 10.1002/mop.10979

Key words: *on-wafer noise source; excess noise ratio; small-signal model; noise temperature; noise parameters*

1. INTRODUCTION

For noise-figure measurements of microwave and millimeter-wave transistors, on-wafer noise sources offer advantages over coaxial noise sources: (i) their effective excess noise ratio (ENR) is directly known at the on-wafer reference plane (plane 22′ in Fig. 1) without requiring an input coaxial-to-on-wafer adapter, therefore, a correction of the input-adapter losses is not necessary and the inaccuracies associated with the measurement of its insertion-loss are reduced; (ii) the ENR level at the on-wafer reference plane is higher, thus reducing noise figure measurement uncertainty. A number of devices have been proposed in the literature as on-wafer noise sources, for example, avalanche diodes [1], resistive devices [2], and Cold-FETs [3]. In [1], the ENR of the avalanche noise diode is computed from its noise temperature, which is measured by using a receiver calibrated with cryogenic and room-temperature standards. In [2], the ENR of the resistive device is obtained by measuring the device noise power with a receiver, whose noise factor has been previously obtained using a commercial calibrated noise source.

In this paper, an alternative method to characterize the ENR of an unmatched avalanche noise diode is presented. It is based on a concept presented in a previous work [3], which consists in extracting a device noise circuit-model from broadband noise and reflection coefficient measurements. The extracted device noise circuit-model includes an intrinsic noise current-source, which is fitted with frequency to obtain an estimation of the device ENR with enhanced accuracy. To determine the device noise model, it is necessary to first obtain the device small-signal model. In the next section, the procedure to measure the noise temperature is described. The avalanche noise model, including the extraction of the equivalent circuit elements, is presented in section 3. The results of the extracted small-signal model and ENR of an avalanche noise diode are presented in section 4. The characterized avalanche noise diode ENR is used to calibrate a noise receiver up to 40 GHz, and the results are also presented in section 4. Finally, some conclusions of the work are presented in section 5.

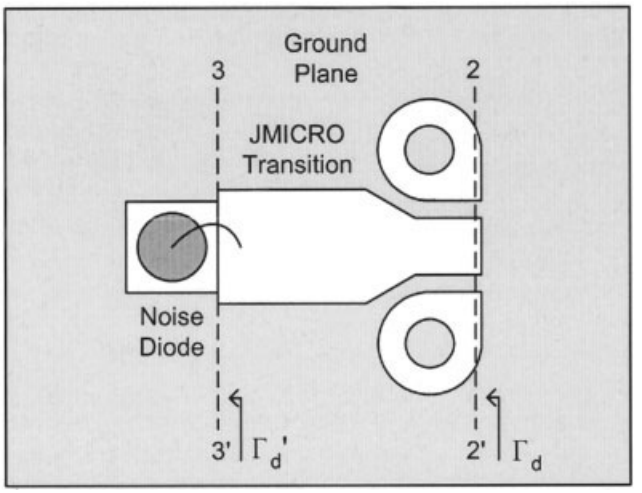

Figure 1 Noise diode wire-bonded to the Jmicro-transition

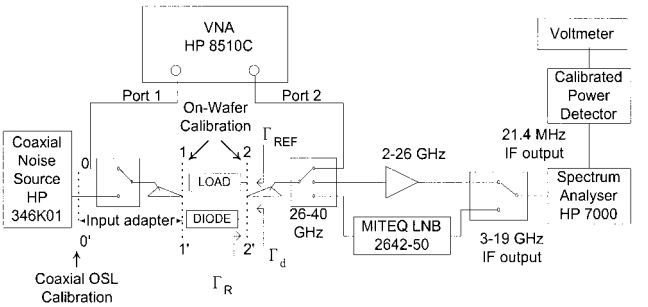

Figure 2 Experimental setup used for characterization of on-wafer avalanche noise diodes

2. NOISE TEMPERATURE MEASUREMENT

The selected device is an avalanche noise diode (NoiseCom NC-406) wire-bonded to the microstrip end of a coplanar-to-microstrip transition from JMICRO Technology (ProbePointTM 1003) (see Fig. 1). The diode bias-point is fixed with a current source. The experimental setup used to characterize the noise diode ENR is shown in Figure 2. Prior to characterizing the noise diode, the receiver noise parameters, referred to by the on-wafer plane 2–2′, are measured using a coaxial noise source via the method proposed in [4].

To determine the diode equivalent noise temperature T_d at plane 2–2′, a passive on-wafer reference load at room temperature T_{REF} (300°K) is connected to plane 2–2′, and its reflection coefficient (Γ_{REF}) and noise power delivered to the receiver (P_{REF}) are measured. Then the diode is connected to plane 2–2′, and its reflection coefficient Γ_d and noise power delivered to the receiver P_d are measured. The equivalent noise temperature T_d is given by

$$T_d = \frac{P_d/\mu(\Gamma_R, \Gamma_d)}{P_{REF}/\mu(\Gamma_R, \Gamma_{REF})} \cdot [T_{REF} + T_R(\Gamma_{REF})] - T_R(\Gamma_d) \qquad (1)$$

where T_R is the receiver noise temperature (evaluated for Γ_{REF} and Γ_d), Γ_R is the receiver input reflection coefficient, and $\mu(\Gamma_R, \Gamma_S) = (1 - |\Gamma_S|^2)/|1 - \Gamma_S\Gamma_R|^2$ is the mismatch coefficient at plane 2–2′.

To refer the noise temperature to the input diode plane (plane 3–3′ in Fig. 1), T_d is translated through the JMICRO coplanar-to-microstrip transition using the following expression:

$$T_d' = \frac{T_d}{G_{av}'} - T_a\left(\frac{1}{G_{av}'} - 1\right), \qquad (2)$$

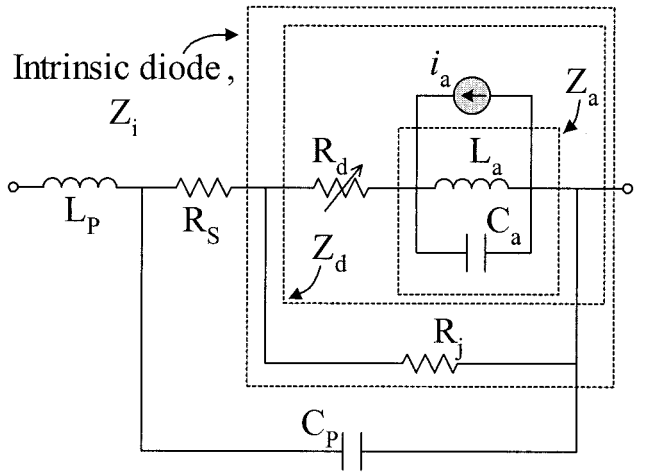

Figure 3 Equivalent circuit of an avalanche noise diode, including an intrinsic noise current source

where T_a is the room temperature (300° K), and G'_{av} is the available gain of the JMICRO-transition computed from its S parameter, estimated by using a model for the JMICRO-transition.

3. AVALANCHE NOISE DIODE MODEL

The diode small-signal equivalent circuit, including an intrinsic noise current-source associated with the avalanche zone i_a [5, 6], is shown in Figure 3. It is assumed that the noise introduced by the contact resistance R_s and the coplanar-to-microstrip transition is thermal noise. The extrinsic and intrinsic elements are determined from diode reflection coefficient measurements at forward-bias and avalanche reverse-bias points, respectively. In both cases, the measured reflection coefficient at plane 2–2′ is translated to the diode plane (plane 3–3′ in Fig. 1), through the JMICRO coplanar-to-microstrip transition.

The extrinsic elements (L_p, R_s, and C_p) are bias independent, and can be computed from the device Z parameters measured under forward-bias conditions $V_d > 0$. Once the extrinsic elements are known, the intrinsic Z matrix Z_i (Fig. 3), is readily identified by de-embedding. The intrinsic elements are extracted from Gilden's analysis [5], where Z_i is expressed by

$$Z_i = \left(\frac{1}{R_j} + \frac{1}{Z_d}\right)^{-1}, \tag{3}$$

where R_j is the depletion zone resistance, and Z_d is the sum of the impedance of the avalanche zone Z_a and that of the drift zone R_d:

$$Z_d = R_d + Z_a; \quad R_d = R_a\left(\frac{1}{1-\frac{\omega^2}{\omega_a^2}}\right)\frac{1-\cos\theta}{\frac{\theta^2}{2}};$$

$$Z_a = \frac{1}{j\omega C_d}\left[\left(1-\frac{\sin\theta}{\theta}\right) + \frac{\frac{\sin\theta}{\theta}+\frac{l_a}{l_d}}{1-\frac{\omega_a^2}{\omega^2}}\right]. \tag{4}$$

In Eq. (4) and the equivalent circuit of Figure 3, R_d is represented by a variable resistance and Z_a by a shunt resonant circuit (L_a and C_a), which are a function of the angular frequency $\omega = 2\pi f$ and the angular avalanche frequency $\omega_a = 2\pi f_a$. R_a is the drift resistance, C_d is the drift capacitance, θ is the transit angle, and l_a/l_d is the relation between length of the avalanche zone and drift zone (in the present work a value of 0.5 is assumed). From Eq. (4), R_d is written in terms of R_a and θ, where $\theta = \omega\tau_d$ and τ_d is the transit time in the avalanche zone. The transit time τ_d and the initial value for R_a are found from measurements at the lower frequency band [5], where $1/R_j$ is negligible in front of $1/Z_d$ in Eq. (3). Then, R_d is approximated by the real part of Z_i, and R_a and τ_d are expressed as

$$R_d(\omega_0) \cong \mathrm{Re}\{Z_i(\omega_0)\}; \quad \theta(\omega_0) = \omega_0\tau_d$$

$$\tau_d = 2R_d(\omega_0)C_d; \quad R_a = \frac{R_d(\omega_0)}{1-\cos\theta_0}\cdot\frac{\theta(\omega_0)^2}{2}\cdot\left(1-\frac{\omega_0^2}{\omega_a^2}\right), \tag{5}$$

where ω_0 is the lowest measurement angular frequency. Also, at the lower frequency band, the imaginary part of Z_i can be approximated by

$$\mathrm{Im}(Z_i) \cong \frac{\omega}{\omega_a^2 C_d} = m\omega, \tag{6}$$

where m is the slope of the imaginary part of Z_i versus ω. Then, an initial value for C_d can be estimated from m:

$$C_d = \frac{1}{\omega_a^2 m}. \tag{7}$$

The angular avalanche frequency ω_a is assumed to be equal to the angular frequency where the imaginary part of Z_i is zero. At this frequency, $\omega = \omega_a$, R_j is calculated from the real part of $Z_i(\omega_a)$, where $1/Z_d$ is negligible. A final adjustment for R_a, C_d, R_j, and f_a is obtained by optimization.

The avalanche current spectral density $\langle i_a^2\rangle$ is expressed as a function of a multiplier factor M, which is assumed to have a smooth frequency dependence [5, 7]:

$$\langle i_a^2\rangle = 2qI_D M^2, \tag{8}$$

where q is the electron charge and I_D is the diode DC-bias current. On the other hand, $\langle i_a^2\rangle$ can be expressed in terms of the diode measured temperature T'_d, and the equivalent circuit elements by taking into account the total diode equivalent noise-current spectral-density $\langle i_t^2\rangle$. In fact, from the diode temperature T'_d and the measured input diode admittance Y_d, the diode equivalent noise current spectral density $\langle i_t^2\rangle$ is computed by using

$$\langle i_t^2\rangle = 4kT'_d\mathrm{Re}\{Y_d\}, \tag{9}$$

where T'_d and Y_d are referred to input diode plane (plane 3–3′ in Fig. 1). Next, $\langle i_t^2\rangle$ is expressed as a function of the diode noise model:

$$\langle i_t^2\rangle = \langle i_{ad}^2\rangle\cdot\left|\frac{Z_a}{Z_d}\cdot\frac{Z_i}{Z_s}\cdot\frac{Z_p}{j\omega L_p + Z_p}\right|^2, \tag{10}$$

where $Z_s = R_s + Z_i$, and $Z_p = Z_s/(1 + j\omega C_p Z_s)$. Then, $\langle i_a^2\rangle$ is computed from Eqs. (9)–(10), and finally M is determined from Eq. (8) at each frequency.

The measured T'_d and, therefore, M are affected by random measurement errors: ENR uncertainty of the coaxial noise source used to calibrate the receiver, input adapter loss determination uncertainty, and noise power measurement uncertainty. According to theoretical predictions [7], M should exhibit a smooth charac-

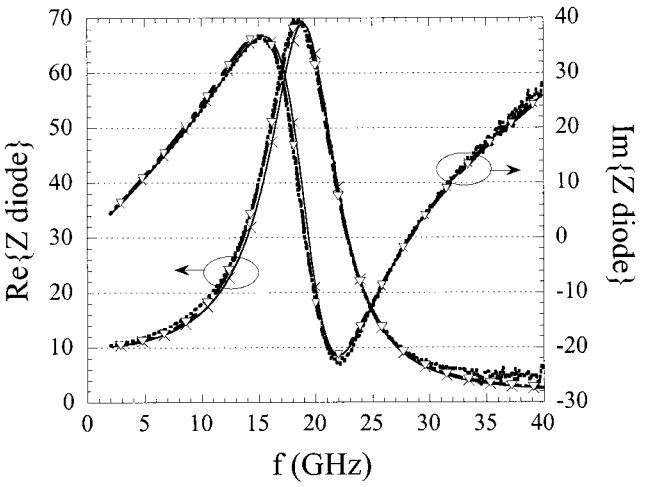

Figure 4 Impedance avalanche noise diode, biased at $V_D = -16.4$ V and $I_D = 16.7$ mA, measured (---), estimated with: initial values (-×-) and optimized values (-▽-)

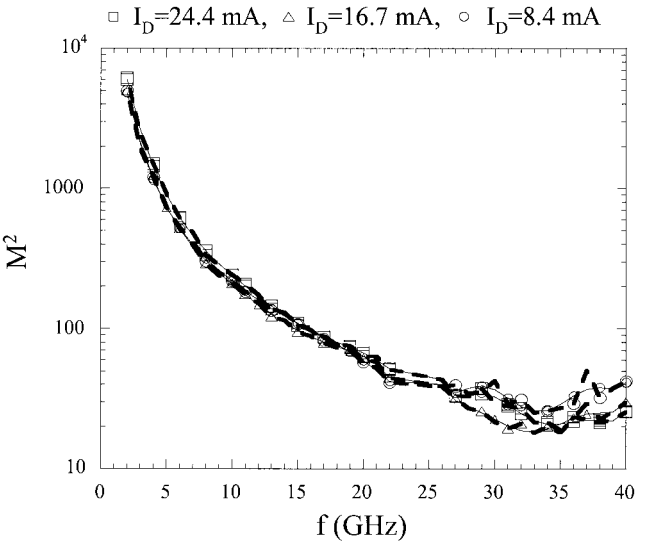

Figure 5 Frequency dependence of multiplier factor M^2, computed from measured T_d (- -) and fitted with frequency (-)

teristic over the frequency. Therefore, it is reasonable to expect a significant accuracy improvement in measured M if a regression technique is applied to M for a sufficient number of frequency points. In this work, we propose the application of a simple regression technique in log scale to the extracted M factor. Then, the noise spectral density $\langle i_t^2 \rangle$ is calculated again, using the fitted multiplier factor M from Eqs. (8) and (10), T'_d and T_d (including the Jmicro-transition), are estimated (T'^{est}_d and T^{est}_d) using Eqs. (9) and (2) respectively, and finally the on-wafer source ENR is calculated from

$$\mathrm{ENR} = 10 \cdot \log\left(\frac{T_d^{est}}{T_0} - 1\right), \tag{11}$$

where T_0 ($=290°$ K) is the standard temperature.

4. EXPERIMENTAL RESULTS

In Figure 4 the avalanche diode admittance measured and estimated, using the initial values and the final optimized values, are compared. In Table 1 the initial and optimized values are presented. The estimated impedance using the initial values shows good agreement with the measured values, and the final optimization is a fine adjustment to the measurements, which minimizes the small differences between both curves.

Figures 5 and 6 show M^2 and the measured ENR (at the on-wafer plane), respectively, as a function of frequency, obtained from measured T_d for several bias points. Applying the previous regression technique, M^2 is fitted with frequency, T_d is estimated,

TABLE 1 Initial and Optimized Values of the Equivalent Circuit Elements of the Avalanche Noise Diode Biased at $V_D = -10.4$ V and $I_D = 16.7$ mA

Elements	Initial Values	Optimized Values
L_p (pH)	165.50	Not optimized
C_p (fF)	160.00	Not optimized
R_s (Ω)	5.43	Not optimized
R_j (Ω)	104.67	102.58
C_d (fF)	180.73	169.44
R_a (Ω)	4.85	4.85
f_a (GHz)	26.55	26.59

and ENR is computed. Fitted M^2 is plotted in Figure 5 and compared to the measurements, while the computed ENR is plotted in Figure 6 and compared to the measurements. Since the adjustment of M^2 is based on a physical noise model, the ripple is strongly reduced, thus allowing the slow variations of ENR with frequency (due to variations of diode output impedance) to be recovered. Therefore, the proposed method reduces ENR measurement uncertainty.

The characterized avalanche noise diode is used as an on-wafer noise source to calibrate the receiver up to 40 GHz, via the procedure described in [8] for noise sources with unrestricted reflection coefficients and applied to the avalanche noise source considered herein. Our results (Fig. 7) agree with those obtained by using a coaxial noise source.

5. CONCLUSIONS

An accurate and inexpensive method to characterize the ENR of on-wafer avalanche diodes, based on determining a noise circuit-model for the diode, has been presented. To reduce uncertainty in the measured noise diode ENR, the intrinsic noise source is fre-

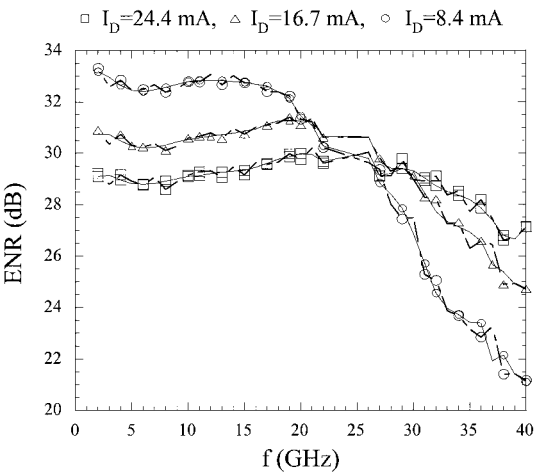

Figure 6 The excess noise ratio, ENR, of an avalanche noise diode at on-wafer plane, measured (- -) and estimated (-)

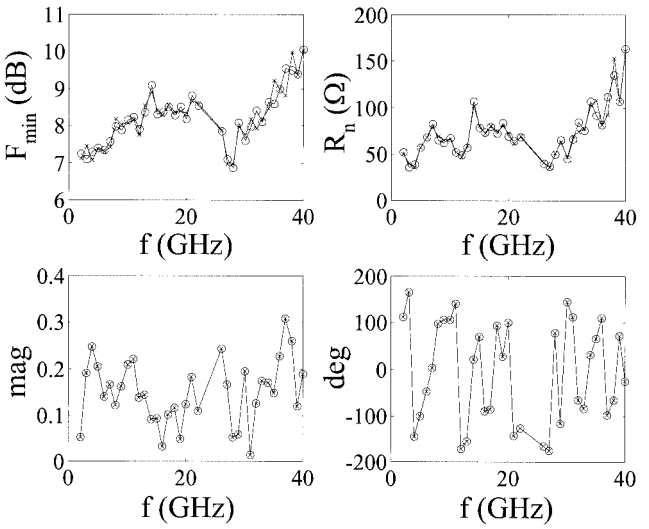

Figure 7 Measured noise-parameters receiver up to 40 GHz, with a coaxial noise-source (○) and avalanche noise diode (×)

quency-fitted according to its smooth frequency dependence. Measured and estimated ENRs are presented, showing a noticeable decrease in the ENR jitter. Also, measured and estimated impedances of the avalanche diode are presented, showing a good agreement. The diode has been used as an on-wafer noise source for calibrating a receiver noise measurement system up to 40 GHz.

ACKNOWLEDGMENTS

This work has been supported by Spanish Government grants TIC2000-0144P4-02, ESP2001-4544-PE, and ESP2002-04141-C03-02, and a scholarship from CONACYT–Mexico.

REFERENCES

1. L.P. Dunleavy, J. Randa, D.K. Walker, R. Billinger, and J. Rice, Characterization and applications of on-wafer diode noise, IEEE Trans Microwave Theory Techn 46 (1998), 2620–2627.
2. P. Béland, S. Labonté, L. Roy, and M. Stubbs, A novel on-wafer resistive source, IEEE Microwave Guided Wave Lett 9 (1999), 227–229.
3. M.C. Maya, A. Lázaro, and L. Pradell, Cold-FET ENR characterization applied to the measurement on-wafer transistor noise parameters, Euro Microwave Conf, 2002, pp 41–44.
4. A. Lázaro and L. Pradell, Extraction of noise parameters of transistor using a spectrum analyser and 50 Ω noise figure measurements only, IEE Electron Lett 34 (1998), 2353–2354.
5. M. Gilden and M.E. Hines, Electronic tuning effects in the read microwave avalanche diode, IEEE Trans Electron Devices 13 (1966), 169–175.
6. M.C. Maya, A. Lázaro, and L. Pradell, Characterization of the excess noise ratio of on-wafer avalanche noise diode, Mediterranean Microwave Symposium, 2002, pp 75–78.
7. R.H. Haitz and F.W. Voltmer, Noise of a self-sustaining avalanche discharge in silicon; studies at microwave frequencies, J App Phys 39 (1968), 3379–3384.
8. A. Lazaro, M.C. Maya, and L. Pradell, Measurement of on-wafer transistor noise parameters without a tuner using a unrestricted noise sources, Microwave J 45 (2002), 20–46.

DESIGN OF A SINGLY-FED CIRCULARLY POLARIZED APERTURE-COUPLED MULTILAYER MICROSTRIP ANTENNA FOR INMARSAT GROUND TERMINAL APPLICATIONS

Yabin Zhang, Binhong Li, and Yijun Liu
Department of Electronic Engineering
Shanghai Jiao Tong University
Shanghai 200030, P. R. China

Received 2 January 2003

ABSTRACT: *This paper presents a design procedure for a singly-fed circularly polarized aperture-coupled multilayer microstrip antenna (SF-ACMMA) for INMARSAT ground terminal applications. In the design, low-cost foam with low permittivity is used for enhancing the impedance bandwidth of antenna. The impedance bandwidth for VSWR ≤ 2 and circular polarization bandwidth for axial ratio (AR) ≤3 dB reach to 18.8% (1.45 to 1.75 GHz) and 12.3%, respectively. A gain of 9.4 dBi is also achieved. These measured results verify the applicability of design.*

 Microwave Opt Technol Lett 38: 92–95, 2003; Published online in Wiley InterScience (www.interscience.wiley.com). DOI 10.1002/mop.10980

Key words: *aperture-coupled; circularly polarized; microstrip antenna*

1. INTRODUCTION

The International Maritime Satellite Organization (INMARSAT) provides worldwide mobile satellite communication services for maritime, land, and aeronautical users. The maritime satellite is a global geostationary Earth orbit (GEO) mobile satellite communication system. The INMARSAT-M system was introduced in 1992 to provide high-quality communications with very small and lightweight terminals, called INMARSAT-Mini-M earth stations. The terminal's receiving and transmission frequency ranges are 1525–1559 MHz and 1626.5–1660.5 MHz, respectively. Its polarization is right-hand circular polarization (RHCP) and its axial ratio is less than 6 dB [1]. In order to use same antenna in Tx/Rx, operation frequency range of candidate antenna should cover both receiving and transmission frequency ranges, namely, 1525–1660.5 MHz. Its fractional impedance bandwidth should be bigger than 8.5%. The fractional bandwidth of a standard microstrip antenna is 2–5%. Therefore, the standard microstrip cannot meet the requirement. An aperture-coupled multilayer microstrip antenna (ACMMA) possesses wide band and, furthermore, 40% fractional impedance bandwidth has been obtained [2]. In addition, this type of configuration has the following advantages [2, 3]:

- the feed network is isolated from the radiating element by the ground plane which prevents spurious radiation;
- an active device can be fabricated on a thin feed substrate with high permittivity for size reduction;
- there is more degree of freedom for the designer.

This type of microstrip antenna was first proposed by David M. Pozar in 1985 [4].

A circularly polarized microstrip antenna can be categorized into two types by its feeding systems: (i) a dual-feed circular polarization antenna with an external polarizer such as 3 dB branch-line hybrid, and (ii) a singly-fed one without a polarizer. Although the dual-fed method can produce broad ellipticity bandwidth, there is usually space constraint. For example, in order to avoid grating lobes, adjacent antenna-element spacing should not